Fatigue resistance of Al-Cu-Li alloys and conventional 7000 and 2000 alloys: notch and environment effects

J.-C. Ehrström[a], O. Andreau[a, b], C. Baudoux[b]

a. Constellium C-TEC, 725 rue Aristide Bergès, 38341 Voreppe Cedex, France, jean-christophe.ehrstrom@constellium.com

b. EDP Institut Pprime, CNRS-ENSMA UPR 3346 – Université de Poitiers – ENSMA, Téléport 2, 1 avenue Clément Ader, 86961 Futuroscope-Chasseneuil Cedex, France

Résumé

The fatigue resistance of an advanced Al-Cu-Li plate alloy (2050) and of conventional alloys 7010 and 2024 is characterized on notched samples (Kt=2.15) with and without an added spark eroded 0.3 mm defect. This characterization is performed in laboratory air, at different frequencies and in vacuum. 2050 always shows a higher fatigue resistance than 7010. The fatigue resistance of 7010 is affected by a relatively coarse constituent particles distribution and a relatively fast fatigue crack growth rate of short cracks. 2024 and 2050 have similar fatigue resistance with no added defect. 2024 offer a slow early fatigue crack growth rate, especially under vacuum.

Mots clés : Fatigue, Aluminium-Cuivre-Lithium, Environnement

1. Introduction

Aluminium – Copper – Lithium alloys, such as those of the AIRWARE® family, show a combination of fatigue resistance, strength and damage tolerance that allows large weight savings in aircraft structures. This weight reduction potential is generally higher than the typically 5% lower density associated with Lithium additions. These new alloys are industrially applied on Bombardier C-Series and Airbus A350. One Al-Cu-Li plate alloy, AA2050, is produced in the largest quantities. The fatigue resistance of AA2050 is similar to the fatigue resistance of high purity 2000 alloys and better than that of 7000 alloys, with a yield stress similar to the yield stress of the latter [1, 2]. This observation holds for tests done on simple open-hole fatigue specimens used for material characterization and on more complex assembled specimens bolted after surface treatment or after surface treatment alone [3, 4].

The improved fatigue resistance of AA2050 versus AA7050 for simple specimens is discussed in [1]: the contribution of a slower early fatigue crack growth rate (FCGR) to this behaviour, in addition to the effect of a more favourable constituent particles distribution, is shown to be significant if not dominant. As the environment affects the low ΔK (stress intensity factor variation in the test) FCGR, the difference in alloy behaviour in absence of any environment effect, i.e. under vacuum, is worth investigating.

The effect of moist air on FCGR is the subject of numerous studies. Petit et al show that it can very well be rationalized when the FCGR is plotted as a function of effective stress intensity factor

normalized by the Young's modulus [5, 6]. Hydrogen is often governing the effect at very low delta_K; an exposition factor depending on the frequency and of the water vapor partial pressure determines the intensity of the effect [7]. The impact of the air humidity on endurance fatigue of Aluminium alloys through its effect on FCGR at low delta_K is particularly emphasized by Bray et al who underline its significance to the industry [8]. The impact of more aggressive environments on endurance fatigue is difficult to assess in relevant laboratory conditions since the corrosion in a long term real exposure is not easily reproduced in the lab [9]. Ricker and Duquette showed that the effect of environment through Hydrogen on endurance fatigue is more pronounced in mode I than in mode III [10].

The present study compares the fatigue behaviour of notched samples of three alloys, 2050 T851, 7010 T7451and 2024T351 in air and vacuum. In some cases, a tiny slot of 0.3 mm is machined at the root of the macroscopic notch to simulate an existing starting crack. In this case, the effect on propagation only is measured.

2. Materials and methods

2.1 Materials

The 2050 T851 plate is 90 mm thick, the 7010 T7451 plate is 110 mm thick and the 2024 T351 is 30 mm thick. The nominal composition of these alloys is given in Table 1.

	Si	Fe	Cu	Mn	Mg	Zn	Ti	Zr	Ag	Li
2050	*0.08 max*	*0.10 max*	*3.2-3.9*	*0.20-0.50*	*0.20-0.6*	-	*0.10 max*	*0.06-0.14*	*0.20-0.7*	*0.7-1.3*
7010	*0.12 max*	*0.15 max*	*1.5-2.0*	-	*2.1-2.6*	*5.6-6.7*	*0.06 max*	*0.10-0.16*	-	-
2024	*0.50 max*	*0.50 max*	*3.8-4.9*	*0.30-0.9*	*1.2-1.8*	-	*0.15 max*	-	-	-

Table 1. *Composition of the alloys*

Constituent size distribution at mid-thickness obtained by optical image analysis is shown in Figure 1: 2050 has significantly less particles compared to 7010. The thinner 2024 plate shows less particles larger than 6 – 9 microns, probably because it particles are broken during rolling. The yield stress of 2050 T851, 7010 T7451 and 2024 T351 in the Long Transverse (LT) is approximately 470 MPa, 450 MPa and 340 MPa respectively.

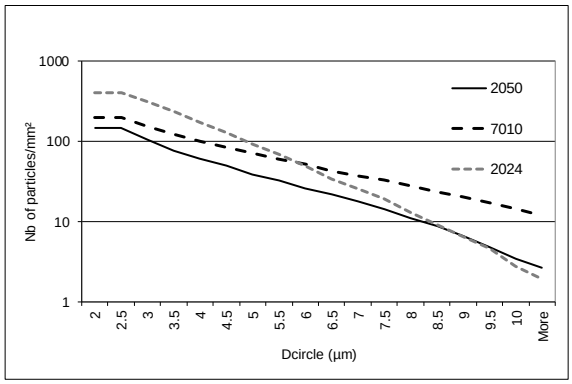

Figure 1. *Distribution in size of constituent particles in the three materials. Dcircle is the diameter of the disk that would have the same surface area as the particle on the micrograph.*

2.2 Testing details

Fatigue samples are extracted from the plate mid-thickness in the LT direction. Two slightly different samples are used because of the size of the vacuum chamber, but their shape is homothetic, and a check showed that both samples give the same results (Figure 2). The stress concentration factor is estimated to Kt=2.15 using Peterson [11].

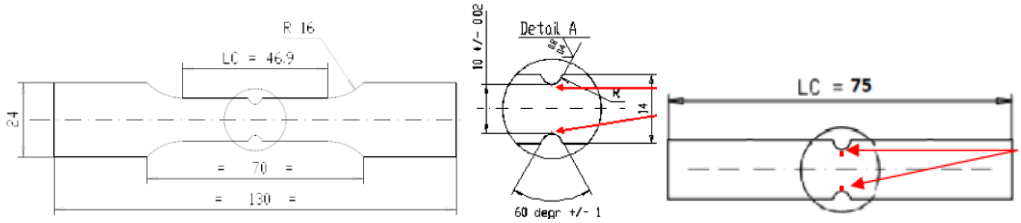

Figure 2. *Fatigue specimens used in air (left) and in vacuum (right). The width is 14 (respectively 9.1) mm, the notch depth and radius is 2 (1.3) mm. A small slot of 0.3 mm depth is spark eroded on each side on some samples.*

The maximum stress is 225 MPa for samples with no small slot, and 150 MPa for samples with a small slot, the target being to obtain fatigue lives not too far from 100000 cycles, the usual reference in the aircraft industry. The R ratio between minimum and maximum stress is 0.5 in order to avoid closure effects. The tests under vacuum were performed at the ENSMA Poitiers. A secondary vacuum of 2*10-5 mBar maximum is imposed at the start of the test, but during the test the pressure can drop to 5*10-7 mBar. The test frequency varies from 0.3 to 15 and 50 Hz

2.3 Crack growth model

In order to better discuss the results with and without the small slot (that are obtained at different applied stresses) a shape of the fatigue curve must be used. For this purpose, a model based on Kujawki estimation of K for a crack starting from a notch is used in combination with a FCGR – ΔK curve fitted by a Forman equation. The model is similar to that presented in [4]. The used Forman coefficients are: $C=1.35.10^{-5}$ mm/cycle, m=2.98 and Kc=115 $MPa.m^{0.5}$. The Wöhler curve aspect prediction for 2024 T3 is shown in Figure 3. For the present purpose that does not require a high precision, the coefficients are not changed for 2050 and 7010 (only the slope of the curve at low ΔK is relevant).

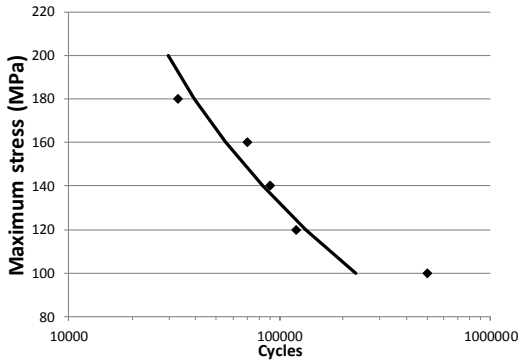

Figure 3. *Comparison of the fatigue crack growth model (line) and the experimental results for 2024 T3.*

3. Test results

The results obtained in air for the three materials are presented in Figure 4. Without the small spark eroded slot, the scatter in life is up to a factor 2 for 2050 T851. 7010 T7451 has a lower fatigue resistance than 2050 T851 and 2024 T351 by a factor 3 associated with a lower scatter. No effect of the test frequency is found. When the small spark eroded slot is present, the overall scatter tends to decrease. As a consequence, 2024 T351 shows a higher fatigue resistance than 2050 T851. 7010 T7451 fatigue resistance remains the lowest.

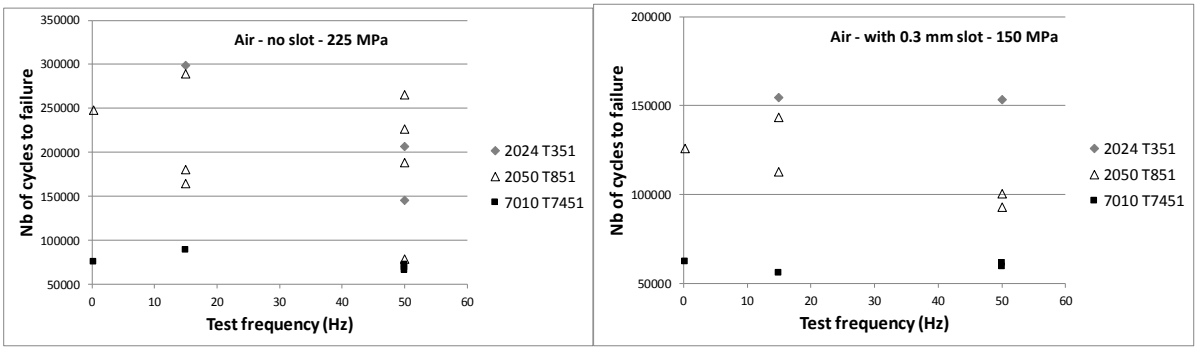

Figure 4. *Fatigue results of tests performed in air, with and without the small 0.3 mm slot. 225 and 150 MPa are the maximum applied stresses.*

Under vacuum, the ranking between the three materials is maintained: 2050 T851 is intermediate between 7010 T7451, which has the lowest fatigue resistance, and 2024 T351, which has the highest fatigue resistance. This holds for tests with slots. The test at 225 MPa maximum stress for 2024 T351 with a slot is lacking, but the test at 150 MPa reached 7000000 without failure. This sample displays a fracture surface that is reflecting light, which is associated with a crystallographic growth [6]. Under this inert environment, the test without slot shows a relatively small difference between the three materials, particularly between 2050 T851 and 7010 T7451.

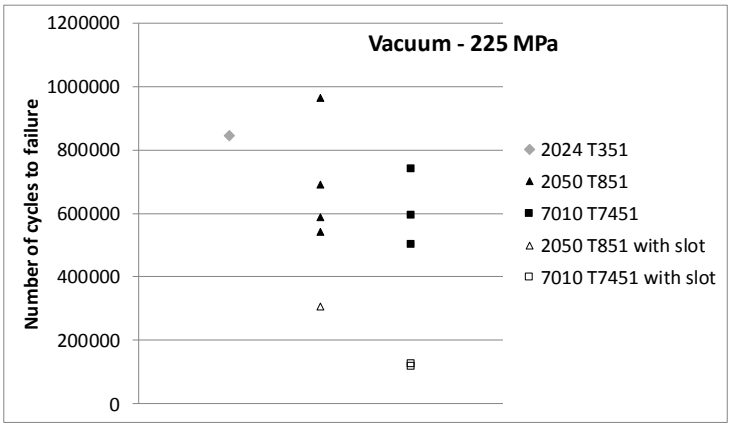

Figure 5. *Fatigue results of the tests performed in vacuum with 225 MPa maximum stress (An additional test at 150 MPa on 2024 T351 reached 7000000 cycles).*

4. Discussion

The results obtained above, plus a few additional, are plotted as Wöhler curves in Figure 6, together with the model curves obtained as shortly described in §2.3 and in more details in [4]. This representation is used to derive approximate stresses for 300000 cycle lives by interpolation or

extrapolation along the slope of the Wöhler curves. This data conversion is used to describe the overall behaviour of the different alloys in a more condensed graph.

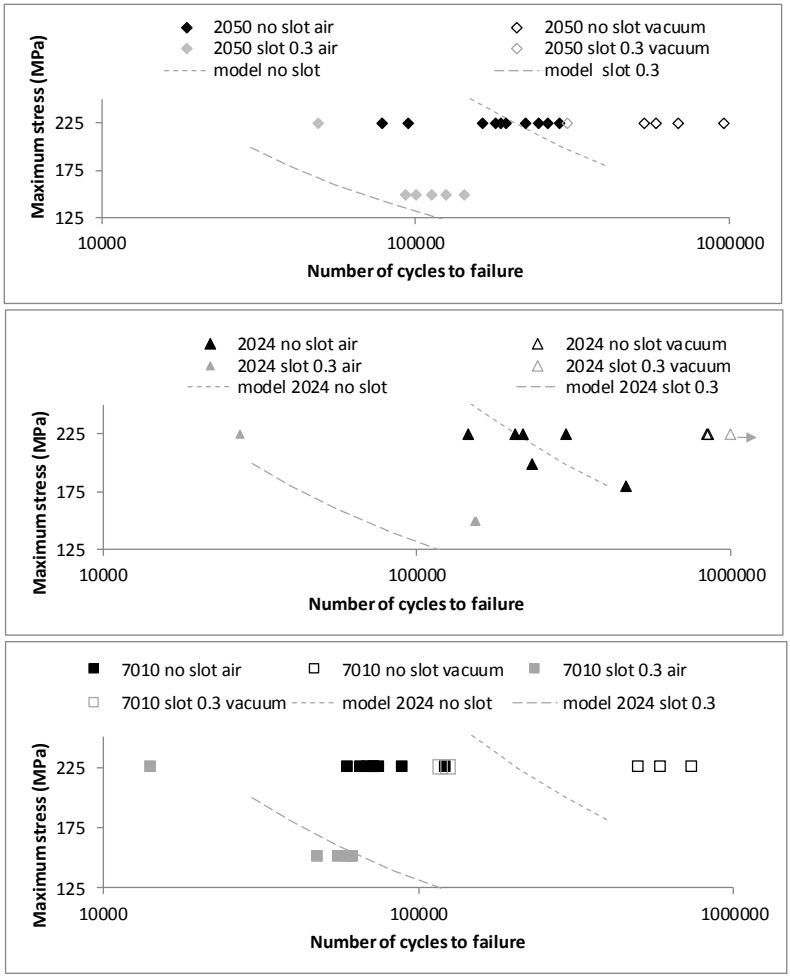

Figure 6. *Data points of fatigue tests presented in a Wöhler diagram together with the slope from the used model.*

The outcome of this data analysis is given in Figure 7, which synthetizes the results for the three materials in all tested conditions. In vacuum with no slot, the fatigue resistance of the three materials is close. When a slot is present, under vacuum, the 7010 T7451 shows the most pronounced drop in fatigue resistance, the 2024 T351 showing almost no decrease. This is associated with the change of cracking mode to a crystallographic mode for 2024 T351. One can conclude that FCGR in vacuum is relatively fast in 7010 T7451.

In air, the 2050 T851 has a similar fatigue resistance to 2024 T351 when no small slot is present. The 7010 T7451 shows the lowest fatigue resistance. Its relatively large particle distribution (Figure 1) explains why this is more pronounced when no slot is present. But the faster FCGR observed in [1] is responsible for the lowest fatigue resistance of 7010 T7451 when the slot is present. The effect of the slot is relatively small in 7010 T7451, which can be explained by the presence of already relatively large initiation defects: the constituent particles. 2024 T351, which has a low yield stress is less affected by the slot, even in air, than 2050 T851. The vacuum effect is large in 2024 T351 with slot (crystallographic mode) and relatively small in 7010 T7451 with slot. It is relatively large in 7010 T7451 without slot, possibly because the initiation life, less sensitive to environment, is shorter than for 2050 T851 and 2024 T351.

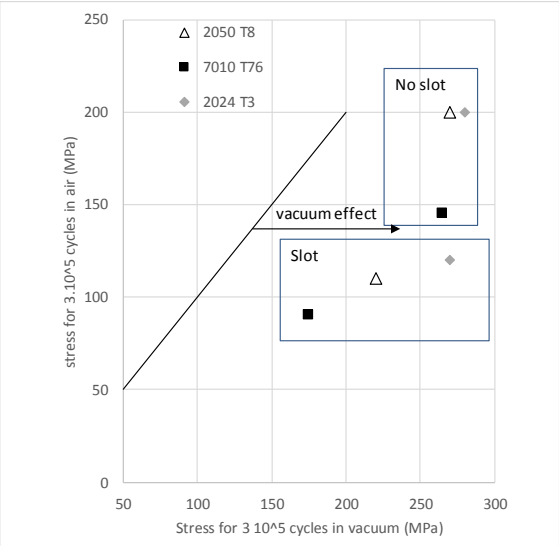

Figure 7. *Synthesis of the average fatigue results in all test conditions for the three materials.*

5. Conclusion

The fatigue resistance of 2050 T851 and conventional aerospace alloys 2024 T351 and 7010 T7451 is characterized with regard to the environment and to the effect of an initial 0.3 mm defect. The fatigue resistance of 2050 T851 is close to the fatigue resistance of 2024 T351 in air and when no slot is present. With a slot, 2024 T351 has a better fatigue resistance than 2050 T851, more so under vacuum.7010 T7451 shows the lowest fatigue resistance. It can be inferred that this is due to the coarser distribution of constituent particles and to a faster short crack FCGR.

The beneficial effect of vacuum is more pronounced when the fatigue starts from a slot, when the life is fully determined by crack growth. It is particularly true when the fracture mode changes to a crystallographic mode, which is the case for 2024 T351 in vacuum with a slot. No effect of frequency is found in laboratory air in the investigated range.

2050 T851 offer a very good compromise between fatigue and strength, with a fatigue resistance that is close to that of 2024 T351except when tested with slot under vacuum, and yield strength that is slightly higher than that of 7010 T7451.

Références

[1] A. Daniélou, J.-C. Ehrström, J.-P. Ronxin, ICAA 13, MMMS/AIME, Warrendale PA 15086 US, 2012
[2] Ph. Lequeu, A. Daniélou, F. Eberl, AEROMAT conference 2007 presentation
[3] J.-C. Ehrström, Matériaux 2010 Nantes, SF2M conference presentation
[4] C. Gasquères, C. Hénon, A. Daniélou, M.-M. Fanget, J.-C. Ehrström, SF2M J. de Printemps 2010
[5] J. Petit, C. Sarrazin-Baudoux, International Journal of Fatigue 32.6 (Jun 2010): 962-970
[6] S. Richard, C. Gasquères, C. Sarrazin-Baudoux, J. Petit, Engng Fracture Mech. 77 (2010) 1941–1952
[7] Y. Ro, S.R. Agnew, G. Bray, R. Gangloff, Mat. Sci. & Engng. A 468-470 (2007), pp. 88-97
[8] G. Bray, R. Bucci and R. Brazill, Materials Science Forum Vols. 331-337 (2000), pp. 1413-1426
[9] R. Dif, J.-C. Ehrstrom Materials Sci. Forum Vols 396 – 402 (2002), pp. 1285 – 1290
[10] R.E. Ricker and D.J. Duquette, ONR Report (1986), Order No. AD-A162627/4/GAR
[11] R.E. Peterson, Stress Concentration Factors, J. Wiley & Sons, New York, 1974